

## Phase delay and group velocity determination at a planar defect state in three dimensional photonic crystals

J. F. Galisteo-López, M. Galli, and L. C. Andreani

*Dipartimento di Fisica "A. Volta," Università di Pavia, Via Bassi 6, 27100 Pavia, Italy*

A. Mihi, R. Pozas, M. Ocaña, and H. Míguez<sup>a)</sup>

*Instituto de Ciencia de Materiales de Sevilla (CSIC-US), Avenida Americo Vesputio s/n, Isla de la Cartuja, 41092 Sevilla, Spain*

(Received 15 September 2006; accepted 27 January 2007; published online 8 March 2007)

Phase sensitive optical transmission measurements have been performed on three dimensional opal-based photonic crystals containing a planar defect. From numerical derivation of the measured phase, the group velocity has been retrieved. Strong modulations in the group velocity are seen to correlate with a recovery in the transmission inside the forbidden spectral interval, demonstrating the presence of a localized defect state. Accordingly, the phase change measured across the forbidden interval doubles in the lattice containing a planar defect with respect to the defect-free crystal, as expected when introducing a localized state inside the pseudogap. All results have been modeled with a scalar wave approximation in a two band model including extinction. © 2007 American Institute of Physics. [DOI: 10.1063/1.2710772]

Photonic crystals<sup>1,2</sup> are acknowledged nowadays as a promising route to control the propagation of electromagnetic radiation as well as to control the emission from embedded light sources via the manipulation of the local density of states. While perfectly periodic systems are known to be suited for multiple applications, introducing local perturbations in their periodicity in a controlled manner allows for the introduction of localized defect states which may be employed to guide light or form ultrasmall optical cavities.<sup>3</sup>

One of the pioneering techniques<sup>4</sup> for the fabrication of three dimensional (3D) photonic crystals operating in the visible and near infrared range is that of self assembly, where monodisperse silica or polymeric colloids naturally form 3D ordered arrays, commonly known as artificial opals. Such technique, with different variations, has also been employed in the growth of samples with controlled defects of several dimensionalities such as point, line, planar, or more complex defects.<sup>5,6</sup>

In this letter we present an optical study of opal-based photonic crystals containing planar defects. By means of a phase sensitive technique, we extract the phase delay as well as the group velocity in the spectral range where the interplay between Bragg diffraction by the ordered lattice and localization at the planar defect is expected to take place. Comparison with the optical response of a bare opal containing no extrinsic defect is used to demonstrate that light is localized within the planar defect structure under analysis and to highlight the different regimes of slow light propagation occurring at band edge and defect state frequencies.

The samples under study consist of artificial opals grown from polystyrene spheres<sup>7,8</sup> (700 nm average diameter and polydispersity of  $\pm 3\%$ ) with and without a planar defect made of TiO<sub>2</sub> nanocrystals, both types being grown on glass substrates. The growth procedure as well as a detailed morphological description of the defective sample can be found in a separate publication.<sup>8</sup> Figure 1 shows scanning electron micrographs (SEMs) of a typical sample containing a defect with different magnifications. Suffice it to say here that this

technique allows for the growth of planar defects with control over its thickness and good quality, thereby allowing for a precise optical study. The real and imaginary parts of the complex transfer function of the sample, which provide information on both the transmission and phase delay, are extracted by means of white light interferometry<sup>9</sup> in a wide spectral range surrounding the *L* pseudogap of the perfectly periodic opal structure.

Experimental results have been modeled by means of the scalar wave approximation (SWA) in a two band model<sup>10</sup> which has proven to reproduce the optical response of different intrinsic and extrinsic colloidal crystal architectures.<sup>8,11</sup> In order to correctly describe the spectral shape of the experimental transmittance, extinction has been introduced by means of a complex component of the refractive index of both the TiO<sub>2</sub> layer ( $n=1.6+0.12i$ ) and the polystyrene spheres [ $n=1.59+\beta i$ , where  $\beta=0.0078+10 \exp(-\lambda/0.12 \times 10^{-6})$  for the opal and  $\beta=100 \exp(-\lambda/0.12 \times 10^{-6})$  for the defective structure]. By doing this, an empirical approach to extinction caused by disorder is introduced. Complex refractive indices have been employed before to account for the effect of structural defects on the optical properties of opals.<sup>12,13</sup> Additionally, a sphere filling fraction of 79%, slightly above the 74% expected for a close packed structure, was estimated from our calculations, a result that is consistent with the sphere interpenetration observed in the SEM.

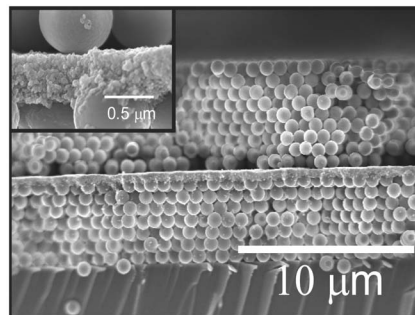


FIG. 1. SEM images of a sample consisting of two opals of seven and nine layers with a defect of 230 nm thick in between.

<sup>a)</sup>Electronic mail: hernan@icmse.csic.es

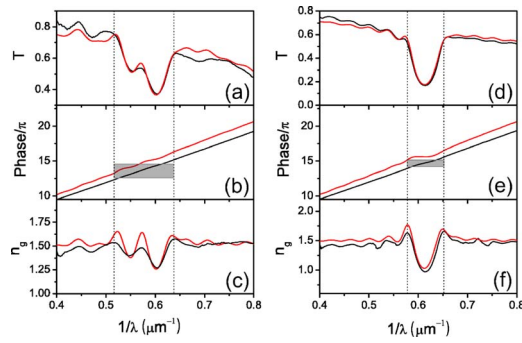


FIG. 2. (Color online) Theoretical (red) and experimental (black) results for samples with and without a planar cavity. Transmission, phase delay, and group index are presented for a 14 layer sample (690 nm spheres) with a 350 nm cavity between the seventh and the eighth [(a)–(c)] and a 15 layer sample (705 nm spheres) [(d)–(f)].

In Fig. 2 we show results of transmittance, phase delay, and group index for colloidal photonic crystals with and without a planar defect. The left panels correspond to samples having the same crystal thickness (seven layers) at both sides of a planar defect of thickness  $d=350$  nm.<sup>14</sup> In the right panels, the same quantities are presented for an opal having 15 layers of spheres, which has a similar optical path if we ignore photonic effects. The overall shape of the transmission spectra is well reproduced by theory for both the bare opal and the defective structure [Figs. 2(a) and 2(d), respectively]. Overimposed on a monotonically decaying transmission caused by diffuse scattering originated by the structural disorder present in the opal matrix,<sup>15</sup> a strong dip in the spectra is found. Such spectral interval, denoted by dashed vertical lines in Fig. 2, corresponds to the  $L$  pseudogap of the opals surrounding the defect. For the case of the sample containing the defect, at a wave number  $1/\lambda=0.57$  ( $\mu\text{m}^{-1}$ ) in the  $L$  pseudogap the transmission recovers, indicating the existence of a localized state associated with the defect through which light may tunnel the structure and be transmitted. The spectral position of the localized state is dictated by the optical thickness of the defect. We have tuned the thickness in order to place the spectral position of the defect state at the center of the  $L$  pseudogap.

Figures 2(b) and 2(e) present both the calculated and experimentally measured absolute phase delays<sup>16</sup> for the two samples under comparison. Further and direct evidence of the existence of a localized state is found in this phase change across the forbidden interval. For the case of the bare opal, the phase change equals  $\pi$ , a behavior also found in one dimensional structures.<sup>17</sup> However, when considering the defective structure, the phase change doubles due to the introduction of a localized state inside the pseudogap. In Figs. 2(b) and 2(e) gray boxes indicate the phase jump across the pseudogap edges, taken from the two maxima in  $n_g$  closest to the dip in transmission and marked by dashed lines (see below). Here it can be seen that the phase delay changes by a value just above  $\pi$  ( $2\pi$ ) for the perfect (doped) structure. The fact that the phase change is slightly larger than the value expected is a finite size effect which eventually disappears when increasing the sample thickness, as we could confirm from our theoretical simulations. The experimental observation of a phase jump of  $2\pi$  between the edges of the pseudogap, in good agreement with theoretical predictions, constitutes an incontrovertible proof of the occurrence

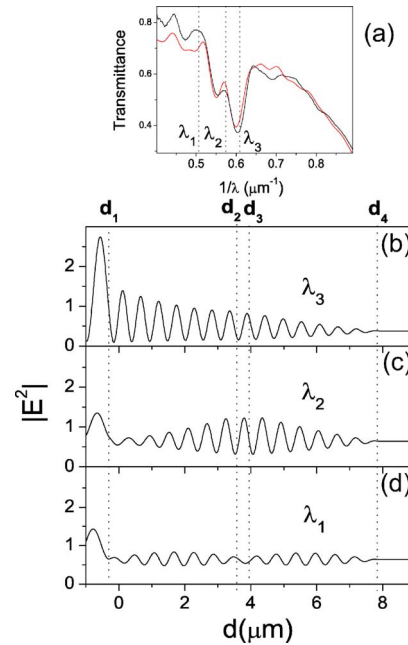


FIG. 3. (Color online) (a) Transmission spectra with several wavelengths highlighted indicating the low energy edge of the pseudogap, the pseudogap and the localized defect state,  $\lambda_1$ – $\lambda_2$ , respectively. [(b)–(d)] Electric field spatial distribution for the aforementioned wavelengths. The vertical dotted lines indicate the air-opal ( $d_1, d_4$ ) and opal-defect boundaries ( $d_2, d_3$ ). The electric field is incident from the left.

of a localized defect state within the nanocrystalline defect coating.

Localization of photon modes within defects in real photonic crystals implies an increase of the time of flight of light through the structure. The group velocity of transmitted light,  $v_g$ , is obtained by means of derivation of the measured absolute phase  $v_g=D(d\omega/d\varphi)$ , where  $\varphi$  is the measured phase and  $D$  the sample thickness, including the number of sphere planes as well as defect thickness.<sup>14</sup> In Figs. 2(c) and 2(f) we plot the group index  $n_g$ , defined as  $c/v_g$ , where  $c$  is the speed of light in vacuum. We obtain high values of  $n_g$ , corresponding to a small group velocity close to the pseudogap edges, analogous to the case of the bare opal.<sup>13,18</sup> As in the case of the bare opal, in the pseudogap region where strong extinction takes place due to Bragg diffraction by the (111) planes, large values of the group index are found for the case of the defect. The fingerprint of the presence of a defect state comes in the shape of a peak of  $n_g$  (that is, a dip of  $v_g$ ) within the forbidden interval, which in our case is observed for  $a/\lambda \approx 0.57$ ,<sup>19</sup> the same spectral position at which the characteristic transmission peak is detected. Such behavior indicates the slowing down of light, which is able to tunnel the sample by means of the localized state associated with the planar defect.

From the results of the group index, shown in Fig. 2(c), it can be seen that the introduction of a planar defect causes a similar reduction in the group velocity as the band bending at the pseudogap edges. However, each type of  $n_g$  maximum is due to a different way of propagation through the crystal. In order to understand the difference between the two scenarios, we have calculated the spatial distribution of the squared electric field for different wavelengths for the case of the defect lattice. The results are plotted in Fig. 3. In Fig. 3(a) we show the three wavelengths considered in the present study;  $\lambda_1$  corresponds to a wavelength at the low

energy pseudogap edge,  $\lambda_2$  to one at the defect state, and  $\lambda_3$  to one inside the pseudogap. In Figs. 3(b)–3(d) vertical dotted lines indicate the air-opal ( $d_1, d_4$ ) and opal-defect ( $d_2, d_3$ ) boundaries. The field impinges from the left. If we consider a wavelength which is contained within the pseudogap [ $\lambda_3$ , Fig. 3(b)], the electric field is exponentially attenuated as it propagates through the sample. As a consequence, a high reflectivity is observed. If the wavelength considered is also contained in the pseudogap but matched now with that of the localized defect state [ $\lambda_2$ , Fig. 3(c)], the electric field is seen to be mainly localized within the defect, between  $d_2$  and  $d_3$ . Finally, for the case of  $\lambda_1$  located at the low energy edge of the pseudogap [Fig. 3(d)], we see how the electric field is evenly distributed across the whole sample. Therefore, although the achieved group velocity for this particular type of sample is similar for the frequencies at the pseudogap edges and the localized defect state, we see how the electric field is mainly localized at the planar defect for the latter. Therefore enhanced light-matter interaction could be achieved by introducing active materials at that location.

Some features observed in the plots of the phase and the group index require further comments. On the one hand the calculated phase overestimates the measured one by  $\sim 7\%$ . On the other hand, stronger oscillations appear in the simulations than in the experiments in the spectral region where the pseudogap and the localized state are found. Regarding the group index, although the overall shape and spectral position of the group index peaks are satisfactorily reproduced by our theoretical model, the amplitude of the features is again overestimated. Such discrepancies arise from the way the sample is described in the theoretical model. The interfaces separating the opal from the air and the defect layer are all modeled as perfectly planar surfaces in the SWA, while in the experiment this is not true. In Fig. 1 we see the opal-air interface consists of a plane of semispheres which have a smaller filling fraction than that of the bulk opal. It shows how the defect layer is asymmetric and presents a planar nature only on one of its sides while on the other side it is interpenetrated with the opal. In the absence of perfectly sharp boundaries, one expects light localization at the planar defect to be smaller, and hence the features of the optical phase, and of the group index, to be less sharply defined. Another possible reason for the observation of such discrepancies is related to the existence of structural disorder. In our simulation we have modeled extinction as absorption by means of a complex component of the refractive index of both spheres and defect layer. Such approach reproduces the transmission spectra, since it accounts for the light not being transmitted, but it fails to correctly reproduce the effect of extinction on the phase and group index. The reason for this is that introducing absorption in the model modifies the effective dispersion of the material via the interaction between the different materials composing the system. On the other hand, the effect of disorder is to fill the forbidden interval with allowed states affecting both the modulus and the phase of the complex transfer function. As a consequence any feature in the optical response due to the existence of the gap, including the phase, will be smeared out as observed experimentally.

Disorder is indeed detrimental for achieving strong light-matter interaction as it diminishes the level of confinement at the defect. Further, a small number of layers can also contribute to reduce light confinement. In order to bring  $n_g$  to a

value above that of the background, and hence obtain enhanced light-matter interaction, one should increase the number of layers of the opals surrounding the defect and increase the sample quality. In fact, increasing the number of layers has been shown to improve the sample quality in the thickness range below 20 layers.<sup>18</sup> Therefore, contrary to what one would think, increasing the number of layers in this range does not boost the effect of disorder. We are currently studying deeper the role of disorder in the present measurements, as well as further developing the growth procedure to improve the sample quality.

In conclusion, we have shown phase sensitive measurements performed on 3D photonic crystals containing defects in the form of a planar cavity. From such measurements we have obtained the absolute phase delay in transmission as well as the group index in a broad spectral region around the pseudogap. Several evidences of the existence of a localized state have been presented such as the recovery of transmission and group index at the frequency of the defect state, as well as a phase jump across the pseudogap which doubles that observed for similar samples in the absence of planar defects.

This work is a result of a collaboration which started within the framework of the COST P11 action “Linear and non-linear optical properties of photonic band gap structures” funded by the European Science Foundation. This work has been partially funded by the CARIPLO Foundation, the Spanish Ministry of Science and Education under Grant No. MAT2005-03028, and by the Ramón Areces Foundation. J.F.G.L. was sponsored by the Postdoctoral Program of the Spanish Ministry of Science and Education.

<sup>1</sup>E. Yablonovitch, Phys. Rev. Lett. **58**, 2085 (1987).

<sup>2</sup>S. John, Phys. Rev. Lett. **58**, 2486 (1987).

<sup>3</sup>J. D. Joannopoulos, R. D. Meade, and J. N. Winn, *Photonic Crystals: Molding the Flow of Light* (Princeton University Press, Princeton, 1995).

<sup>4</sup>C. López, Adv. Mater. (Weinheim, Ger.) **15**, 1679 (2003).

<sup>5</sup>P. V. Braun, S. A. Rinne, and F. Garcia-Santamaria, Adv. Mater. (Weinheim, Ger.) **18**, 2665 (2006).

<sup>6</sup>A. Arsenault, F. Fleischhaker, G. von Freymann, V. Kitaev, H. Míguez, A. Mihi, N. Tétreault, E. Vekris, I. Manners, S. Aitchison, D. Perovic, and G. A. Ozin, Adv. Mater. (Weinheim, Ger.) **18**, 2779 (2006).

<sup>7</sup>J. F. Galisteo-López, E. Palacios-Lidón, E. Castillo-Martínez, and C. López, Phys. Rev. B **68**, 115109 (2003).

<sup>8</sup>R. Pozas, A. Mihi, M. Ocaña, and H. Míguez, Adv. Mater. (Weinheim, Ger.) **18**, 1183 (2006).

<sup>9</sup>M. Galli, F. Marabelli, and G. Guizzetti, Appl. Opt. **42**, 3910 (2003).

<sup>10</sup>K. W. Shung and Y. C. Tsai, Phys. Rev. B **48**, 11265 (1993).

<sup>11</sup>D. M. Mittleman, J. F. Bertone, P. Jiang, K. S. Hwang, and V. L. Colvin, J. Chem. Phys. **111**, 345 (1999).

<sup>12</sup>J. F. Galisteo-López and W. L. Vos, Phys. Rev. E **66**, 036616 (2002).

<sup>13</sup>G. von Freymann, S. John, S. Wong, V. Kitaev, and G. A. Ozin, Appl. Phys. Lett. **86**, 053108 (2005).

<sup>14</sup>The number of sphere planes as well as the defect thickness may be obtained from the fitting of the experimental transmission spectra with the SWA, which has been shown in Ref. 8 to provide a good agreement.

<sup>15</sup>Y. A. Vlasov, M. A. Kaliteevski, and V. V. Nikolaev, Phys. Rev. B **60**, 1555 (1999).

<sup>16</sup>A proper normalization procedure was followed, as in Ref. 17, in order to remove any spurious contributions to the phase coming from the glass substrate.

<sup>17</sup>M. Galli, D. Bajoni, F. Marabelli, L. C. Andreani, L. Pavesi, and G. Pucker, Phys. Rev. B **69**, 115107 (2004).

<sup>18</sup>J. F. Galisteo-López, M. Galli, M. Patrini, A. Balestreri, L. C. Andreani, and C. López, Phys. Rev. B **73**, 125103 (2006).

<sup>19</sup>Notice that in the present case the fcc lattice constant has a value of  $a \sim 1 \mu\text{m}$ , so that all wave number values given can be regarded as the commonly employed reduced frequency  $a/\lambda$ .